Ann. Occup. Hyg., Vol. 52, No. 1, pp. 9–21, 2008
Published by Oxford University Press
on behalf of the British Occupational Hygiene Society
doi:10.1093/annhyg/mem056

Ultrafine and Respirable Particles in an Automotive Grey Iron Foundry

DOUGLAS E. EVANS[1], WILLIAM A. HEITBRINK[2]*, THOMAS J. SLAVIN[3] and THOMAS M. PETERS[2]

[1]Division of Applied Research and Technology, National Institute for Occupational Safety and Health, 4676 Columbia Parkway, MS-R3, Cincinnati, OH 45226, USA; [2]Department of Occupational and Environmental Health, University of Iowa, 102 IREH, 100 Oakdale Campus, Iowa City, IA 52242-5000, USA; [3]International Truck and Engine Corporation, 4201 Winfield Road, Warrenville, IL 60555, USA

Received 6 April 2007; in final form 9 October 2007; published online 3 December 2007

Ultrafine particle number and respirable particle mass concentrations were measured throughout an automotive grey iron foundry during winter, spring and summer using a particle concentration mapping procedure. Substantial temporal and spatial variability was observed in all seasons and attributed, in part, to the batch nature of operations, process emission variability and frequent work interruptions. The need for fine mapping grids was demonstrated, where elevations in particle concentrations were highly localized. Ultrafine particle concentrations were generally greatest during winter when incoming make-up air was heated with direct fire, natural gas burners. Make-up air drawn from roof level had elevated respirable mass and ultrafine number concentrations above ambient outdoor levels, suggesting inadvertent recirculation of foundry process emissions. Elevated respirable mass concentrations were highly localized on occasions (e.g. abrasive blasting and grinding), depended on the area within the facility where measurements were obtained, but were largely unaffected by season. Particle sources were further characterized by measuring their respective number and mass concentrations by particle size. Sources that contributed to ultrafine particles included process-specific sources (e.g. melting and pouring operations), and non-process sources (e.g. direct fire natural gas heating units, a liquid propane-fuelled sweeper and cigarette smoking) were additionally identified.

INTRODUCTION

Increased cardiopulmonary morbidity and mortality has been associated with exposure to ambient fine particulate matter, usually measured as the mass concentration of particles <2.5 μm (Dockery *et al.*, 1993; Samet *et al.*, 2000; Brook *et al.*, 2004). Evidence suggests that ultrafine particles (diameter < 100 nm) may drive this relationship because they may be considerably more toxic than larger particles found in ambient particulate matter (Oberdörster, 2001; Donaldson *et al.*, 2002; Oberdorster *et al.*, 2002; Englert, 2004; Gilmour *et al.*, 2004; Nel, 2005). Although number concentration is often dominated by ultrafine particles, their mass is often negligible compared to that of larger particles (Maynard, 2003). Consequently, regulatory standards based on mass concentration may not be protective of individuals from either an environmental or an occupational health perspective.

Ultrafine particle exposures may be generated by 'hot' processes (Vincent and Clement, 2000), such as welding (Brouwer *et al.*, 2004), and by combustion, such as burning of fuel in internal combustion engines (Ramachandran *et al.*, 2005). Consequently, exposure to ultrafine particles may be common in industrial workplaces where these processes occur. Möhlmann and Riediger (Riediger and Möhlmann 2001; Möhlmann, 2005) observed elevated ultrafine particle concentrations ranging from 2×10^4 to 4×10^7 particles cm^{-3} near various processes including plasma cutting, metal inert gas and tungsten inert gas welding, metal grinding, aircraft maintenance, brazing, food preservation (smoking), smelting and laser ablation. During primary aluminium production, Thomassen *et al.* (2006) identified ultrafine particle concentrations

*Author to whom correspondence should be addressed.
Tel: +1-319-335-4213; fax: +1-319-335-4225;
e-mail: william-heitbrink@uiowa.edu

ranging anywhere from 1.5×10^3 to 8.0×10^4 particles cm^{-3} in a crane operator's cab receiving clean filtered air, to 1.0×10^7 particles cm^{-3} adjacent to anode changing operations within a pre-bake potroom.

The concentration, composition and size of particles may differ substantially depending on their underlying source. For example, in automotive machining environments, wet machining, dry machining and grinding with straight oils may produce markedly different aerosol properties (Dasch *et al.*, 2005). In addition, ultrafine particles produced at relatively high concentration from non-process sources, such as direct-fired natural gas heating systems (Peters *et al.*, 2006; Heitbrink *et al.*, 2007), may mask process-related sources. Foundry operations include numerous potential sources of ultrafine particles which may range from melting, pouring and shakeout (Chang *et al.*, 2005) to metalworking activities such as grinding (Zimmer and Maynard, 2003) and welding (Zimmer and Biswas, 2001; Brouwer *et al.*, 2004). In consequence, adverse health outcomes from potentially diverse aerosol exposures may therefore vary substantially. A careful assessment of aerosol emissions and underlying sources is therefore required within these workplace environments.

Objectives

With automated processes and manufacturing operations, an understanding of contaminant emission sources is required before planning to assess worker exposure to ultrafine and respirable particles. Understanding emission sources is also critical to implementing effective and targeted control strategies to reduce potential exposures. The primary objective of this work was to identify notable emission sources in a grey iron foundry. This objective was achieved through the mapping of ultrafine particle number and respirable mass concentrations. A secondary objective was to obtain number and mass concentrations according to particle size for identified sources.

Facility and process descriptions

Measurements were conducted within a 0.5 million square feet automotive grey iron foundry located in Indianapolis, IN, USA. Three work shifts poured >700 tons of iron alloy per day, sufficient to supply three diesel engine machining and assembly facilities with cast cylinder blocks and heads. Although not physically partitioned, the foundry was divided into the following three distinct operational areas.

Core and mould area. Cores and moulds functioned as temporary internal voids and the outermost form of a casting, respectively, as hot molten alloy was poured into the assembly. Thus, the final shape of the casting was determined by these internal and external components. As castings sufficiently cooled and solidified, both mould and core materials were disintegrated and removed. Cores were made of new silica sand, coated with a resin, mechanically pressed into shape and cured by forcing a catalyst gas through it. External moulds were formed of 'green sand' composed of reconditioned sand, sea coal, clay binder and sufficient moisture to hold its shape when compressed. Presses were occasionally cleaned with compressed air and patterns were sometimes sprayed with a mould release agent. Cores were coated on appropriate surfaces in automated processes, with a water-based wash containing aluminium and magnesium silicates in addition to small amounts of silica and carbon. Components were subsequently conveyed through an electrically heated oven to bake the core wash, which primarily served to prevent burn-in of the sand by the molten alloy during pouring. Core and mould components were fully assembled and transported to the pour operations by conveyors.

A worker's breakroom was situated next to the core–mould area. During breaks, distinctive cigarette smoke aromas were evident on occasions in this locale. Furthermore, several small gas-supplied heating units were also noted close to the roof within this area and served to temper incoming make-up air during cold periods.

Melt and pour area. Iron ingots, scrap metal and additives were charged into any of eight induction furnaces and melted to produce molten grey iron alloy. The molten alloy from the furnace was decanted into vessels, or ladles, mounted to overhead cranes that transported the molten material to holding furnaces, which in turn transferred the iron into either an automated pouring machine (the rotopour) or manually manipulated ladles for hand pouring. Alloy was poured into mould assemblies to form engine blocks, cylinder heads and other engine components. Upon pouring, components were moved along enclosed, ventilated conveyers to the shakeout–cleaning area.

Although exact alloy composition was proprietary information, cast components met specifications for ASTM (American Society for Testing and Materials) class 35 grey iron designation. SAE (Society of Automotive Engineers) grades G3500 or G4000 grey cast iron may achieve ASTM class 35. With iron as the matrix, base compositions for these grades may range from 3.0 to 3.5% total carbon, 0.6 to 0.9% manganese, 1.3 to 1.8% silicon, together with relatively minor components of phosphorus and sulphur (ASM, 1983).

During furnace charging, fugitive emissions were observed to rise with thermal plumes, towards large exhaust vents within a cupola at roof level. Emissions were particularly noticeable during furnace charging and during pouring when furnaces were tilted to transfer molten alloy into crane-mounted ladles. During normal operation, some fume avoided capture by local exhaust ventilation shrouds mounted to the lid of the furnaces. However, tilting the furnace during pouring

caused obvious emissions into the workplace. Upon pouring the molten alloy (1430–1445°C) into the mould assembly, visible fume and a lazy flame were observed from combustion and thermal degradation of components within the core–mould assemblies. Although local exhaust ventilation was situated to capture most of these emissions from the pouring process, some fugitive emissions occurred.

Shakeout and cleaning area. Once iron was poured into the mould assembly, it was conveyed along a lengthy enclosed path where it cooled while continuing to give off fugitive emissions. Although most sections of ventilated enclosure appeared to control emissions, some small sections provided incomplete dust control and noticeable emissions. When sufficiently solidified and cooled, the mould assembly was moved to a vibrating conveyor that separated the mould and core material from the casting. However, the ventilation system for the conveyor did not completely capture emissions. Emissions appeared to consist of partial combustion products (observed as smoke) and dust generated by mechanically separating the mould and core materials from the castings. In addition, several small gas-supplied heating units were also noted close to the roof within the shakeout–cleaning area. Castings underwent further cleaning by automated shot blasting followed by an automated coarse, dry grinding to remove unwanted cast material. Finally, cast components were visually inspected and, if needed, additional manual chipping and grinding was performed.

METHODS

Particle concentration mapping

Ultrafine particle number and respirable mass concentrations were measured throughout the facility following the mapping procedures of Peters *et al.* (2006). Briefly, a condensation particle counter (CPC, Model 3007, TSI Inc., Shoreview, MN, USA) was used to measure the number concentration of particles with diameters from 0.01 to 1 μm. The upper concentration limit of the CPC was extended by using a dilutor consisting of a modified high efficiency particulate air filter cartridge with a pre-drilled end cap (Peters *et al.*, 2006). An optical particle counter (OPC, PDM-1108, Grimm, Ainring, Germany) was used to measure particle number concentration of particles from 0.3 to 20 μm. Respirable particle mass concentrations C_{Resp} were computed as follows:

$$C_{\mathrm{Resp}} = \sum_{i=1}^{12} \frac{\pi}{6} \rho f_i d_i^3 C_i, \qquad (1)$$

where

f_i = fraction of respirable particles in channel i computed per American Conference of Governmental Industrial Hygienists (ACGIH) criteria (ACGIH, 2007),
d_i = geometric mean of the upper and lower boundaries for channel i (μm),
C_i = particle number concentration in channel i of the OPC and
ρ = assumed unit density of 1 g cm^{-3}.

Ultrafine particle number concentrations (N_{UFP}) were computed as follows:

$$N_{\mathrm{UFP}} = N_{\mathrm{CPC}} - \sum_{i=1}^{5} C_i, \qquad (2)$$

where

N_{CPC} = particle number concentration measured with the CPC.

As the lower boundary from the OPC's first channel was 0.3 μm and the upper boundary of the fifth channel was 1 μm, N_{UFP} is strictly the number concentration of particles in the 0.01- to 0.3-μm range. However, subsequent measurements of particle number concentration by size presented here illustrate that particle counts are generally dominated by ultrafine particles (<0.1 μm), with particles in the 0.1- to 0.3-μm range subsequently comprising a relatively small fraction. Therefore as a practical matter, N_{UFP}, is essentially the number concentration of ultrafine particles (<0.1 μm).

In addition to the aerosol instruments described, an indoor air quality monitor (Q-Track Plus, Model 8554, TSI Inc.) was used to provide temperature, relative humidity, CO_2 and CO data during spring and summer.

During the winter mapping in December 2004, data for the maps were collected over two consecutive days. This consisted of two coarse sampling grids on the first day with between 59 and 102 sampling locations and one fine sampling grid on the second day, with 192 locations. During the summer mapping in August 2005, one mapping session was conducted per day, for three consecutive days and the three mapping exercises involved between 54 and 247 locations. One additional coarse mapping event (98 locations) took place during late March 2005, and provided useful insights into particle source identification. However, the spring mapping event was not included in any statistical analyses, as one single-mapping event in spring cannot be statistically compared with equal weighting to three mapping events in winter and summer.

Comparison of OPC-estimated to gravimetrically measured respirable mass concentration

Gravimetric samples were collected concurrently with the real-time aerosol measurements during mapping events and at fixed locations in the foundry with a respirable sampler (4.2 Lpm, GK2.69 Respirable

Cyclone, BGI, Waltham, MA, USA). Battery-operated pumps (Universal Sampler pumps, Model 224-PCXR4, SKC, Eighty-Four, PA, USA) were used to draw air through the filter-based mass samplers at their specified flow rates. Pumps were pre-calibrated with a flow calibrator (tri-Cal, BGI). If the sampling flow was deviated by >5% from the initial set point, the pump ceased sampling and displayed the elapsed time. Filters from these samplers were analysed gravimetrically using National Institute for Occupational Safety and Health (NIOSH) method 0600 (NIOSH, 1998).

Particle size distribution measurements

During summer, particle size distributions were measured with an electrical low pressure impactor (ELPI, Dekati Ltd, Tampere, Finland) and the OPC, together with a CPC for ultrafine particle concentration measurements, at a select number of locations according to Fig. 4 and described in Table 3. ELPI particle number concentrations by size were measured every second in 12 channels from 0.007 to 10 μm over a period of at least 5 min, as a single event at each location. Particle mass concentration by size was derived from OPC data, as the OPC had a larger upper particle size limit than the ELPI and the OPC had been routinely used to derive respirable mass concentrations in the prior mapping events and in our prior studies (Peters *et al.*, 2006; Heitbrink *et al.*, 2007). Furthermore, mass concentrations obtained from the ELPI may be adversely influenced by the diffusion of smaller particles to the uppermost stages of the ELPI cascade impactor, since by particle mass, particles of larger diameter carry a much greater weighting. This phenomenon has been noted when monitoring combustion aerosols of small size, but at relatively high concentrations (Maricq *et al.*, 2000, 2006; Gulijk *et al.*, 2004; Kinsey *et al.*, 2006).

Statistical analyses

Mapping exercises resulted in multiple concentration measurements within each area. Analyses of variance (ANOVAs) (Proc GLM, SAS, Cary, NC) were conducted to determine whether season (winter or summer) or area (core–mould, melt–pour and shakeout–cleaning) or their interaction influenced ultrafine particle number or respirable mass concentration. All statistical procedures were conducted with the geometric mean of log-transformed concentrations within each area for each mapping event to avoid issues of spatial and temporal autocorrelation. Season was subsequently found not to influence respirable mass concentration; therefore, winter and summer data were combined for these analyses and Tukey's studentized range test multiple comparison test, using the variance estimated from the ANOVA, was used to examine differences between the mean log-transformed concentrations in the different areas. However, season was the only variable found to influence ultrafine particle number concentration; therefore, Tukey's test was not required.

The geometric mean ratio of OPC-derived estimates, divided by the measured gravimetric mass concentration, was computed along with upper and lower confidence limits. Regression analyses were used to evaluate whether OPC-estimated mass concentrations were predictive of those measured gravimetrically, according to the following model and regression coefficients and R^2, the fraction of variability in C_{Grav} that is explained by C_{Resp} was obtained:

$$Y = a + bX + \epsilon, \tag{3}$$

where

$Y = \ln(C_{Grav})$ and C_{Grav} is the mass concentration measured gravimetrically (mg m^{-3}),
$X = \ln(C_{Resp})$ and C_{Resp} is the mass concentration estimated from the OPC (mg m^{-3}),
a and b are regression coefficients and
ϵ is the residual, the difference between the observed and modelled value of gravimetric concentration.

The SAS General Linear Models Procedure was used to compute 95% confidence intervals about the values of the regression coefficients. This model was selected to evaluate whether the OPC estimates of respirable dust concentration were directly proportional to the gravimetric measurements.

RESULTS AND FINDINGS

Comparison of OPC-estimated to gravimetrically measured respirable mass

Figure 1 provides a plot comparing respirable mass concentration derived from OPC estimates to those of gravimetric filter-based samples. In Fig. 1, the regression equation is expressed in terms of a power law model. From the regression analysis, the value

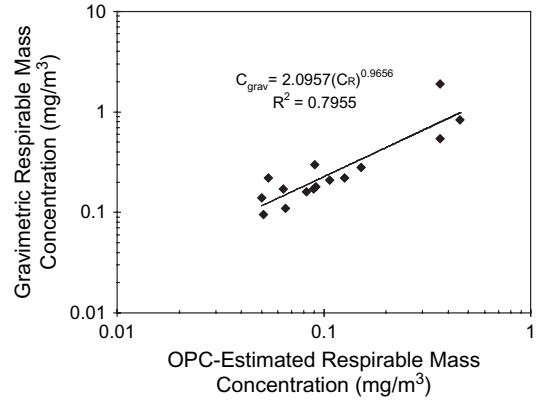

Fig. 1. Comparison of respirable mass concentration from OPC estimates to gravimetric measurements.

of b and its 95% confidence interval is 0.96 ± 0.34. This indicates that the OPC response is, within the limits of experimental error, proportional to the gravimetrically measured concentration. The value of the regression coefficient a, and its 95% confidence interval was 0.74 ± 0.79. The value e^a, of 2.1, is essentially the proportionality constant between the gravimetrically measured respirable dust concentration and the estimate of respirable dust concentration obtained from the OPC. The geometric mean ratio of respirable mass concentration obtained from the OPC to gravimetric measurements was 2.3 with upper and lower 95% confidence limits of 2.8 and 1.7, respectively. Thus, OPC response is proportional to respirable mass concentration, although the OPC underestimates the respirable mass concentration by a factor of approximately two.

Particle concentration mapping

Tables 1 and 2 summarize data for ultrafine particle number and respirable mass concentration data, respectively, and Figs 2 and 3 present concentration maps of these metrics. Maps were constructed from data obtained during the winter, spring and summer mapping events as noted. Each map corresponded to a single data collection event, during which both particle number and respirable mass concentration were simultaneously measured at numerous locations.

Ultrafine particle number concentration. Ultrafine particle number concentration maps (Fig. 2) illustrate the high degree of temporal variability of ultrafine particle concentration within the foundry. These concentration maps have different peak concentrations during each mapping event. Ultrafine particle number concentration was significantly less in summer than in winter ($P = 0.002$), as visually evident in Fig. 2. However, process area and the interaction between process area and season did not significantly affect geometric mean number concentration ($P = 0.24$ and 0.14, respectively) and therefore, the results of Tukey's test were not required in Table 1, which presents the geometric mean of ultrafine particle number concentration by season and area.

Respirable mass concentration. Respirable mass concentration maps (Fig. 3) indicated considerable variability between individual mapping events, with largely inconsistent localized elevated concentrations noted in the core–mould, melt–pour and shakeout–cleaning areas of the facility. ANOVA determined that both the season and the interaction between season and process area ($P = 0.12$ and 0.62, respectively) did not influence respirable mass concentration significantly. However, process area did influence respirable aerosol concentration ($P = 0.007$). A multiple comparison test on the combined data and the results of the multiple comparison tests are presented in Table 2 with the summary statistics for respirable mass concentration by season and area. Overall, the melt–pour area had a significantly higher respirable mass concentration than either the core–mould or the shakeout–cleaning areas.

Occupational exposure to respirable crystalline silica is a potential health concern and it is an

Table 1. Ultrafine particle number concentration by area during winter, spring and summer within the foundry

Area	Winter		Spring	Summer	
	Geometric mean (particles cm^{-3})	Geometric standard deviation	Geometric mean (particles cm^{-3})[a]	Geometric mean (particles cm^{-3})	Geometric standard deviation
Core–mould	2.39×10^5	1.13	2.30×10^5	7.01×10^4	1.49
Melt–pour	2.09×10^5	1.57	1.75×10^5	1.68×10^5	1.61
Shakeout–cleaning	2.15×10^5	1.65	2.76×10^5	7.10×10^4	1.81

[a]Geometric mean from multiple measurements taken within one single-mapping event in spring. In contrast, geometric means for winter and summer derived from mean of multiple measurements in each area and from three separate mapping events.

Table 2. OPC-estimated respirable mass concentration by area during winter, spring and summer within the foundry

Area	Winter		Spring	Summer		Multiple comparison test grouping code[b]
	Geometric mean (mg m^{-3})	Geometric standard deviation	Geometric mean (mg m^{-3})[a]	Geometric mean (mg m^{-3})	Geometric standard deviation	
Core–mould	0.05	1.19	0.15	0.07	1.16	B
Melt–pour	0.09	1.30	0.10	0.10	1.13	A
Shakeout–cleaning	0.05	1.48	0.12	0.07	1.11	B

[a]Geometric mean from multiple measurements taken within one single-mapping event in spring. In contrast, geometric means for winter and summer derived from mean of multiple measurements in each area and from three separate mapping events.
[b]Comparison was only performed between data from winter and summer as statistical analyses determined that both season and area influenced respirable mass concentration. Spring data were not included in the analyses, as only one single-mapping event was performed.

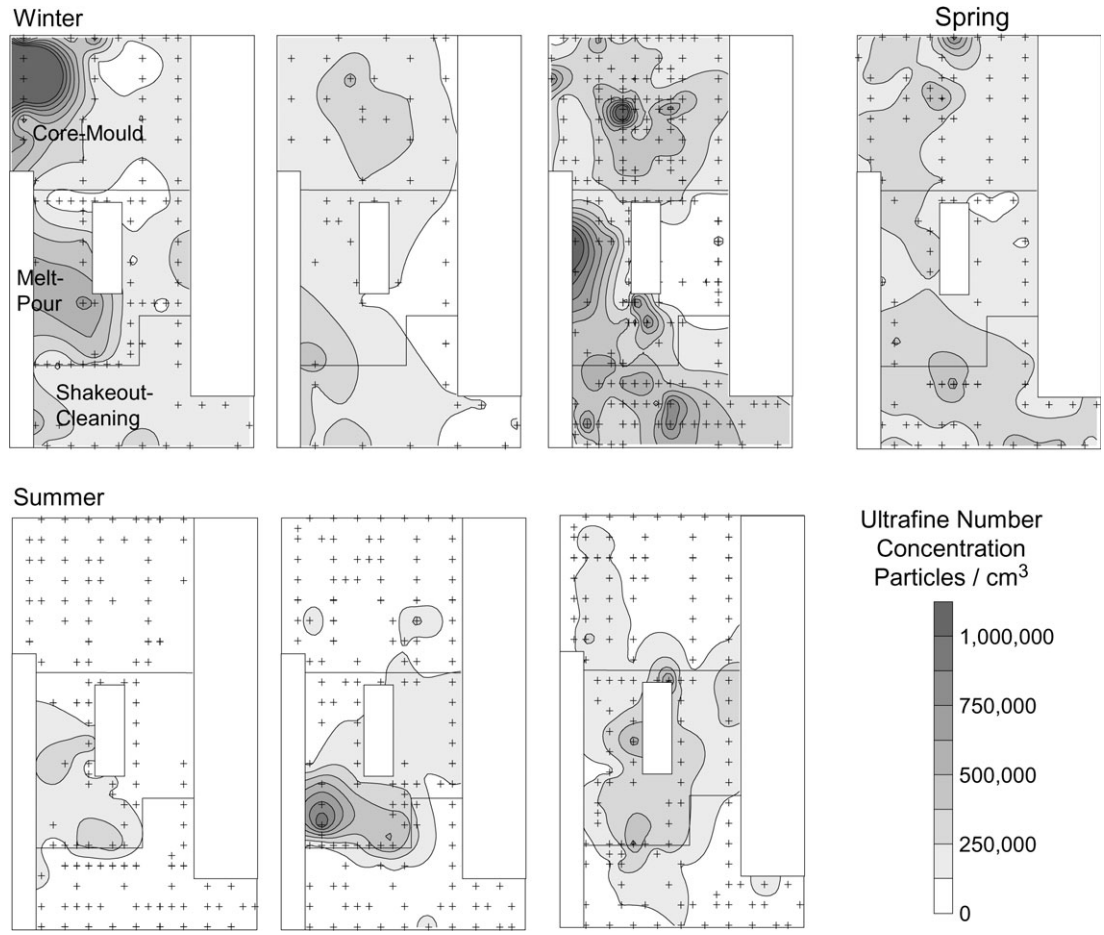

Fig. 2. Ultrafine particle number concentration in winter, spring and summer. Crosses indicate measurement locations.

important dust control consideration within this foundry. ACGIH (ACGIH, 2007) has stated a threshold limit value of 0.025 mg m^{-3} for respirable crystalline silica. However, this study was not conducted with an aim to assess worker's exposure to crystalline silica. Respirable mass concentrations presented in Table 2 and Fig. 3 ranged anywhere from 0.001 to 1.07 mg m^{-3}, but it is unclear how crystalline silica or any other single constituent contributed to these estimated concentrations.

Particle size distribution measurements

Figure 4 provides measurement locations further described in Table 3. Figure 5a provides number concentration by size and Fig. 5b provides mass concentration by size for general locations, outdoor backgrounds and incoming make-up air. Figure 6a provides number concentration by size and Fig. 6b provides mass concentration by size for processes, sources and incoming make-up air. In general, particle number concentration by size differed according to the underlying particle generation process or location. Most mass distributions exhibited two modes, with one centred near 0.4 μm and the other at ∼5 μm (Figs 5b and 6b). The measurement obtained near the abrasive blasting process (Fig. 6b) was an exception, with an additional mass mode centred on 1 μm, whereas other measurements tended to indicate particle mass concentration minima close to this particular particle size. This abrasive blasting process also exhibited elevated particle number concentrations (Fig. 6a) at larger particle diameters (i.e. >1 μm) compared to many other processes.

Particle number and mass concentrations measured outdoors were substantially lower than any measurements taken within the foundry (see locations c and d in Table 3 and Fig. 5). Although the facility make-up air (location a in Table 3 and Figs 5 and 6) was the cleanest air sampled within the foundry, it appeared contaminated when compared to that measured outdoors at ground level (locations c and d in Fig. 5a,b).

Measurements obtained above the rotopour and within the plume of the propane sweeper had elevated particle number concentrations in the smallest channel (0.007–0.023 μm) measured by the ELPI (Fig. 6a). The sweeper contributed elevated ultrafine concentrations in the core–mould and melt–pour

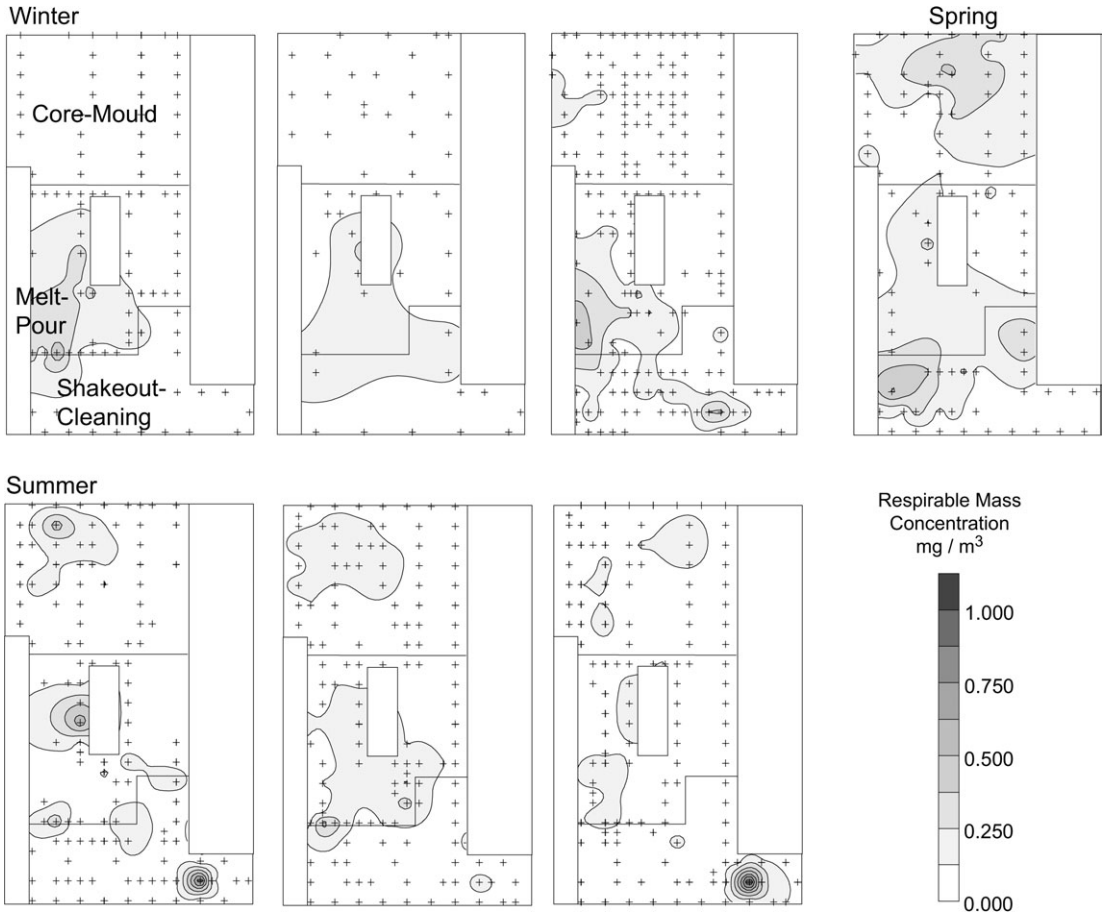

Fig. 3. Respirable mass concentration in winter, spring and summer. Crosses indicate measurement locations.

areas on occasions (see elevation in Fig. 2a winter map 1, top left hand corner). The rotopour operation generated the greatest particle concentrations by number or by mass, with three possible modes ($<$0.02, $\sim$0.035 and $\sim$0.2 μm) evident in the particle number by size distribution (Fig. 6a). In contrast, near other foundry processes, the smallest mode in the particle number by size distribution occurred in the next largest size channel (0.023–0.031 μm). The rotopour operation generated the greatest particle concentrations by number or by mass, with three possible modes ($<$0.023, $\sim$0.035 and $\sim$0.2 μm) evident in the particle number by size distribution (Fig. 6a). Compared to particle number concentrations in the incoming make-up air, the concentrations measured on the melt deck were substantially elevated for all particles sizes (Fig. 6a).

DISCUSSION

Comparison of OPC-estimated to gravimetrically measured respirable mass

Respirable mass concentration estimated with the OPC was substantially less than, but proportional to, that measured with the gravimetric samplers. Simply stated, the OPC underestimated respirable mass concentration by a factor of 2.3 based upon the geometric mean ratio of OPC estimate of respirable mass concentration to gravimetrical measured respirable mass concentration. A similar 2-fold underestimate was observed in an engine machining and assembly facility, where metalworking fluid mists were encountered (Heitbrink *et al.*, 2007). Optical aerosol instrument response is known to vary with particle properties (Gebhart, 2001), including density, morphology, refractive index and other optical properties. These particle properties were likely to have varied widely throughout the foundry, influenced by predominant particle sources. Nevertheless, OPC estimates of respirable mass concentration provide useful indications of 'relative' mass concentration within workplaces, where their cost, portability and rapid measurement capability make them amenable to use in applications, where relative concentrations are needed.

Particle concentration mapping

Concentration mapping is an exploratory and measurement intensive procedure to illustrate

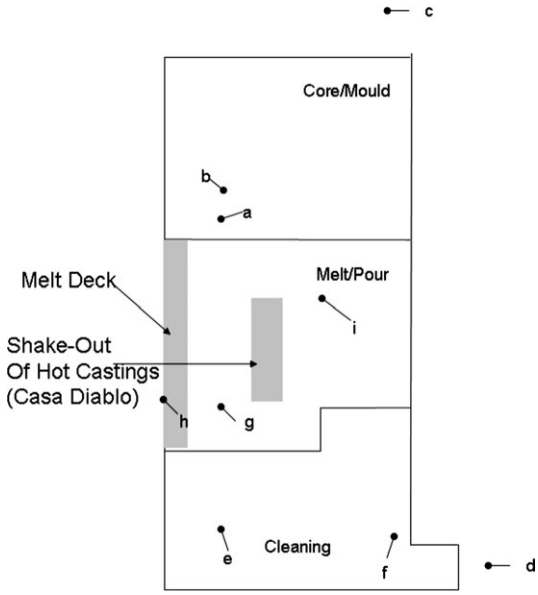

Fig. 4. Foundry floor plan with process and location areas identified. A more detailed description of all locations identified with letters is provided in Table 3. Position codes: a, make-up air; b, core–mould; c, outdoor background NE; d, outdoor background SE; e, shakeout–cleaning area; f, abrasive blasting/grinding; g, rotopour; h, melt deck; i, propane sweeper background and propane sweeper plume. Shake out of hot castings (Casa Diablo) fully enclosed, and operated with forced ventilation under negative pressure.

contaminant variability within a workplace but is unlikely to find routine practice in occupational hygiene, due to the extensive data collection and subsequent processing involved. However, concentration maps may be useful as powerful visual aids in informing facility staff and management of high concentration areas where control measures need improvement. Concentration maps may also indicate the relative magnitude and the extent that contaminants migrate from their original point of emission to other areas of the plant. Thus, concentration maps may be useful for planning exposure-assessment studies and for estimating personal exposures to ultrafine particles in the absence of exposure measurements and where worker location is known. Presently, personal exposure monitors for ultrafine particles are not widely available and workplace ultrafine particle concentrations may span perhaps four orders of magnitude (i.e. 1×10^3 to 1×10^7 particles cm^{-3}).

The utility of mapping will largely depend upon the consistency of the plant's operations. For intermittent batch operations, different mapping events revealed noticeably different areas of peak concentration as illustrated by the respirable mass concentration maps in summer (see Fig. 3) and ultrafine particle concentration maps in Fig. 2. In addition, others have reported that foundry emissions vary considerably even within the same process (Chang *et al.*, 2005). A combination of several mapping events reported here aided in identifying the majority of particle emission sources within the foundry facility, their relative positions and magnitudes and extent of contaminant migration from the point of emission. Although with hindsight, this may have been improved with finer sampling grids, particularly at source locations.

Emission sources

Concentration mapping revealed several obvious and less obvious sources of both ultrafine and respirable particulate. Melting and pouring of alloy into moulds created obvious emissions of respirable and ultrafine particulate matter. Pouring molten alloy into transfer ladles created a visible plume of freshly generated fume which rose towards the roof of the foundry into a cupola, where exhaust fans were located. The pouring of molten alloy into moulds caused combustible materials in the mould assembly to burn, releasing thermal decomposition products. Although engineering controls (enclosures with exhaust ventilation) were present, these did not appear to completely capture fugitive emissions. For example, carbon monoxide measurements taken upon the rotopour deck (~20 ppm, the highest reading attained) suggested that particle plumes were likely influenced by partial combustion. Chang *et al.* (2005) reported that a pouring operation together with subsequent shakeout contributed to the highest concentration emissions for both gases and particles. The ultrafine particle concentration in the plume from the rotopour was $\sim 8.4 \times 10^5$ particles cm^{-3}, which is likely an underestimate, since the ambient temperature of 45°C exceeded the maximum operating temperature of 35°C for the CPC (TSI, 2004). In addition, the number and mass concentrations by size measured at the rotopour exceeded all others. In Fig. 6a, the particle number by size distribution for the fume generated at the rotopour appeared to possess three modes. The smallest and dominant mode (<0.023 μm) was likely composed of freshly nucleated particles, some indication of a possible intermediate mode, observed at ~0.04 μm, and the largest size mode (~0.2 μm) likely formed by condensation of volatiles onto pre-existing particles.

Alloy melting was an obvious source of ultrafine particles. In Table 3, this resulted in the highest ultrafine particle number concentration observed, 1.6×10^6 particles cm^{-3}, as measured with CPC and OPC. On the melt deck, the mode in the particle number by size distribution occurred on the 0.023- to 0.0301-μm impaction stage as opposed to the 0.007–0.023 μm for the rotopour operation. On the melt deck, however, measurements could not be conducted directly within the thermal plume, for safety considerations. Two major modes were present in the mass distributions measured on the melt deck

Table 3. Summary data for locations, processes, sources and facility make-up air, where simultaneous aerosol size distributions were obtained in summer

Position codes (see Fig. 4 for positions within facility)	Name	Description	Ultrafine[a] particle number concentration (particles cm^{-3})	OPC-estimated respirable mass concentration (mg m^{-3})
a	Make-up air	Incoming air drawn through ducts from roof level	6.69×10^4	0.035
b	Core–mould	Centre of core/mould production area	1.18×10^5	0.081
c	Outdoor background NE	Measurements taken 10 m from the north-east corner of foundry	3.30×10^4	0.013
d	Outdoor background SE	Measurements taken 5 m from the south-east corner of foundry	3.69×10^4	0.008
e	Shakeout–cleaning area	Centre of cleaning area. Some fugitive emissions from hot engine cylinder heads observed	1.71×10^5	0.036
f	Abrasive blasting/grinding	Measurements taken where engine blocks exited abrasive blasting and grinding operations	3.51×10^4	0.099
g	Rotopour[b]	Adjacent to operator station above pour operation; molten alloy poured into mould/core assemblies; fugitive emissions observed but mostly controlled by strong exhaust ventilation	8.42×10^5	0.187
h	Melt deck	Adjacent to operator station ~5 m from furnace	1.60×10^6	0.093
i	Propane sweeper background	In the melt/pour area adjacent to Casa Diablo prior to sweeper measurements	7.73×10^5	0.070
i	Propane sweeper plume	2–3 m behind but within the exhaust plume from a liquid propane gas-fuelled sweeper	1.09×10^6	0.091

See size distributions provided in Figs 5a–6b.
[a]'Ultrafine' particle concentration consists of particles in the 10- to 300-nm range, based on simultaneous measurements with the CPC and OPC. See equation (2).
[b]CPC may have underestimated particle counts, due to an ambient air temperature in excess of 45°C.

(Fig. 6b). The mass mode associated with particles <1 μm closely matched that of the incoming make-up air. However, the mass mode composed of particles > 1 μm was substantially elevated above that of the incoming make-up air and, therefore, these particles were likely generated within the foundry facility. It is unclear whether these particles may have been generated by the melting and furnace operations alone or by other nearby processes, as no physical barriers existed between processes or operations.

Other less obvious sources of ultrafine particles were not directly related to foundry processes. Significant non-process-related particle sources included the intermittent operation of small roof-level direct gas-fired heating units during cooler months, to warm incoming make-up air, the use of a liquefied propane gas-fuelled sweeper and cigarette smoking. Direct gas-fired heating has been shown to generate substantial quantities of ultrafine particles (Peters *et al.*, 2006; Heitbrink *et al.*, 2007). The particles generated by these gas heaters were generally dispersed throughout the facility with prevailing air currents through forced ventilation, resulting in ultrafine particle number concentrations of $\sim 2 \times 10^5$ particles cm^{-3} during winter throughout the foundry, as compared to summer measurements of $\sim 0.7 \times 10^5$ particles cm^{-3} in the core–mould and in the shakeout–cleaning areas (see Table 1). In addition, the elevated particle number concentration spot, in the centre of the core–mould area (Fig. 2, winter mapping event 3), was due to a series of measurements taken in close proximity to an air duct, bringing contaminated air directly from a heating unit. In contrast, respirable mass concentrations did not vary with season with the operation of the gas-fired heaters, in this, or in our previous studies (Peters *et al.*, 2006; Heitbrink *et al.*, 2007) (see Table 2). Particle number and mass concentration by size measurements, for similar natural gas-fired heating units, are reported in Heitbrink *et al.* (2007).

The sweeper was periodically used to remove dust and debris deposits from accessible floor spaces and walkways. Together with high ultrafine particle number concentrations, the sweeper exhaust plume additionally contained elevated CO concentrations, with

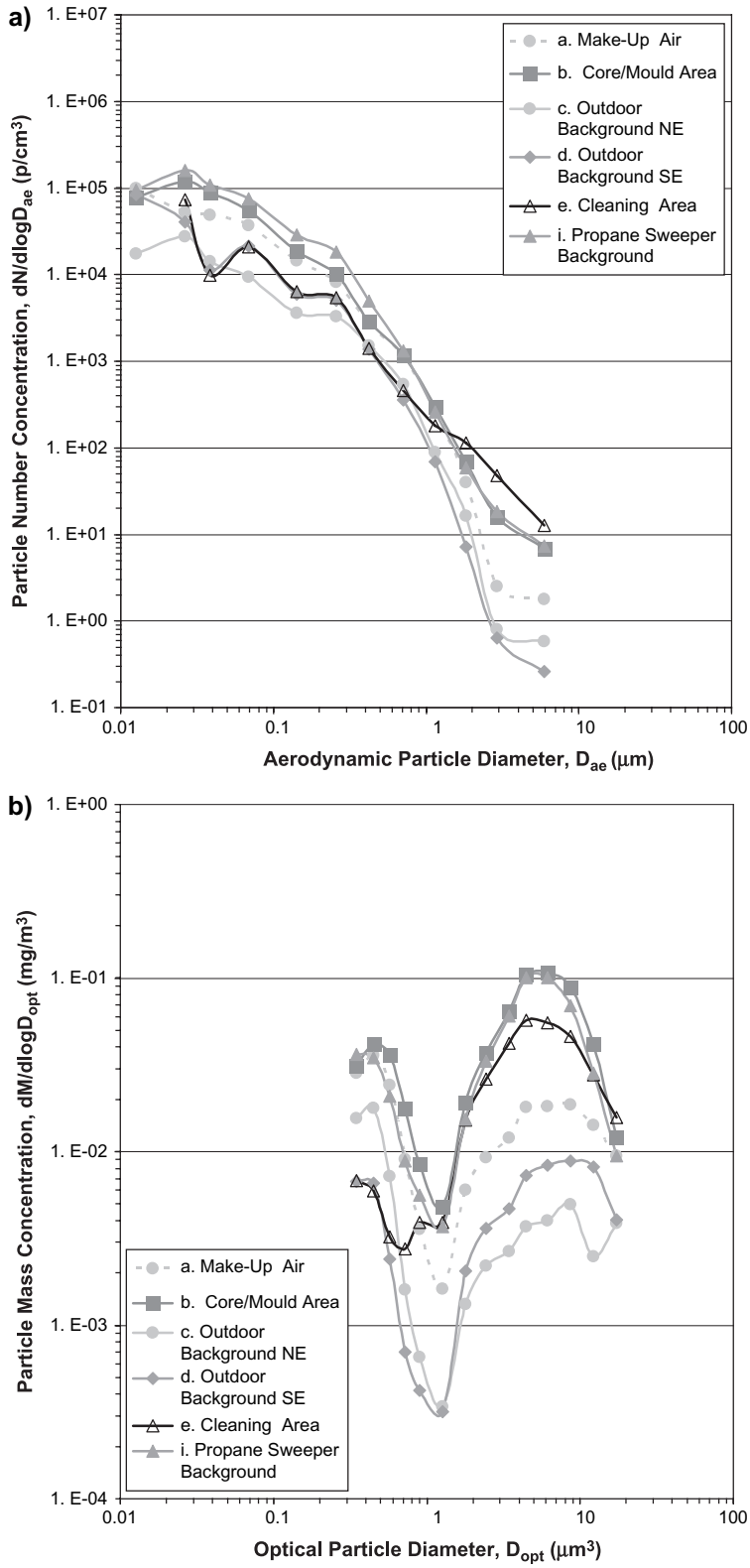

Fig. 5. (a) Particle number concentration by size measured with the ELPI and (b) particle mass concentration by size measured with the OPC for general locations, outdoor backgrounds and incoming make-up air. See Table 3 for additional details and Fig. 4 for physical locations within the facility.

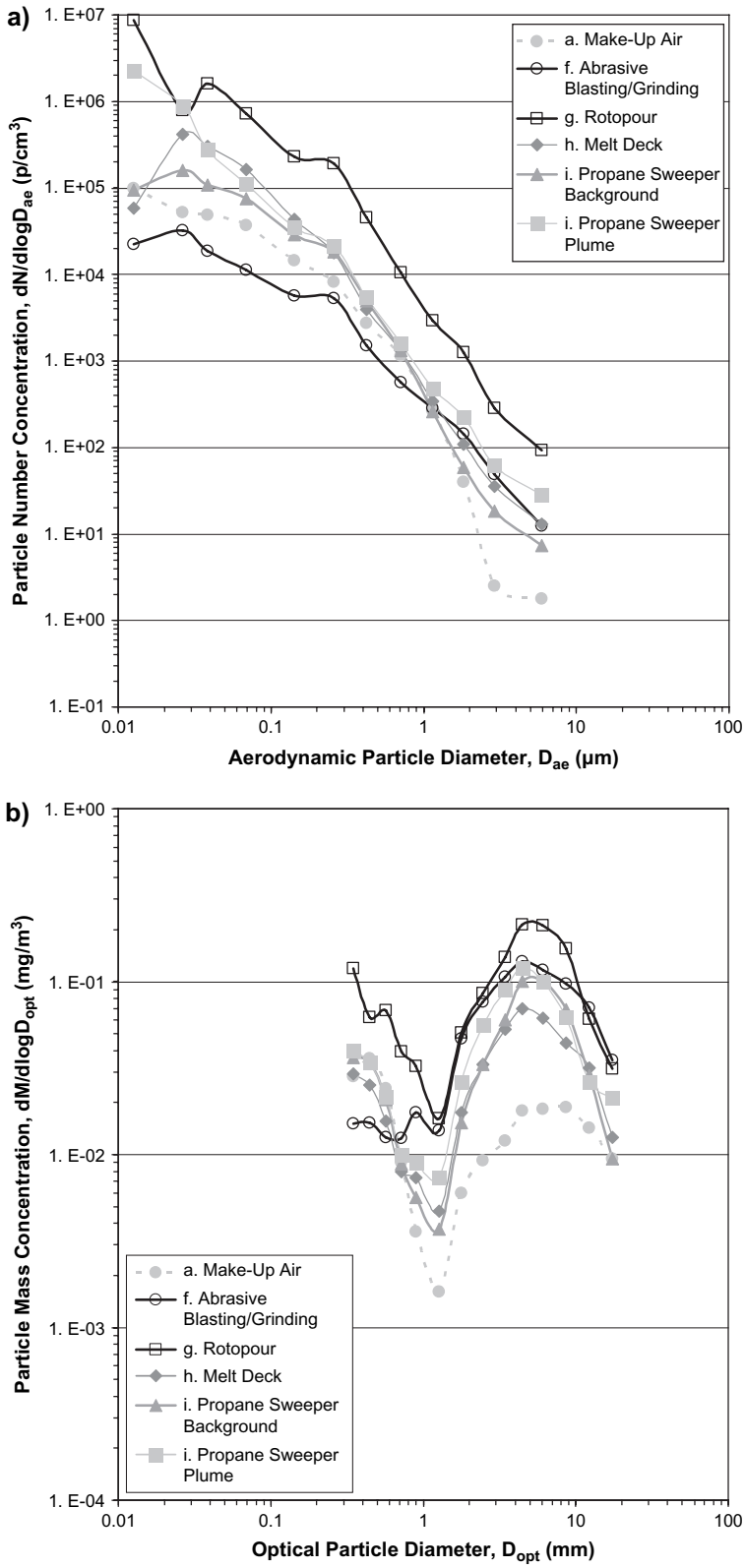

Fig. 6. (a) Particle number concentration by size measured with the ELPI and (b) particle mass concentration by size measured with the OPC for processes, sources and incoming make-up air. See Table 3 for additional details and Fig. 4 for physical locations within the facility.

105 ppm being the peak reading attained. Although an important non-process source of ultrafines, the sweeper was encountered only occasionally (for example, Fig. 2, winter mapping event 1, ultrafine elevation in top left hand corner). For particles <0.05 μm, ultrafine particle number concentrations in the sweeper's exhaust plume were much greater than prior background measurements (see Fig. 6a). In addition, small elevations in particle mass concentration by size also indicated that larger particle resuspension from the functioning sweeper may have also occurred. Staff at the facility are currently considering an electrical sweeper when a replacement for this vehicle is due.

In the vicinity of a worker rest area and nearby, a distinct aroma of cigarette smoke was evident. Ultrafine particle number concentrations were also simultaneously elevated. It is highly likely that this source was responsible for the ultrafine particle number concentration rise, in the area noted (Fig. 2, spring map, top centre). No other obvious ultrafine particle sources were apparent. Smoking has since been banned throughout this facility.

Particle size distributions measured in make-up air (Fig. 6a,b) were similar to those observed indoors and different from those measured outside the facility. This observation suggests that the make-up air may have been contaminated (both ultrafine and respirable mass) by inadvertent recirculation of air exhausted from the facility. The geometric mean of ultrafine particle number concentration in the mould/core area and in the shakeout–cleaning area were 7.0×10^4 and 7.1×10^4 particles cm^{-3}, respectively, as compared to 6.7×10^4 particles cm^{-3} in the incoming fresh air (Table 4). In relatively clean areas of the plant, ultrafine aerosol concentration may be explained by the aerosol present in the supplied make-up air, in addition to the ingress of cleaner outdoor air, particularly during summer, due to open doors and windows.

CONCLUSIONS

Ultrafine particle number and respirable mass concentration varied both spatially and temporally within an automotive grey iron foundry, in contrast to virtual steady-state conditions encountered in an adjacent engine machining facility. Respirable mass concentrations ranged from 0.001 to 1.07 mg m^{-3} and the ultrafine particle number concentration ranged from 1.9×10^4 to 3.5×10^6 particles cm^{-3}. Temporal variability was attributed to the batch nature of particle-generating activities such as melting and pouring, variability in process emissions and frequent work interruptions. Spatial and temporal variability require that particle mapping efforts be conducted on a more frequent and spatially resolved basis to accurately determine particle concentrations, identify sources and indicate the extent of contaminant migration from them.

Alloy melting and subsequent pouring operations were the primary sources of ultrafine particles within the foundry. Non-process foundry sources substantially influenced indoor ultrafine particle number concentration. Specific non-process aerosol sources included direct fire natural gas heaters, liquefied propane-fuelled sweeper trucks and cigarette smoking. Elevated ultrafine particle number concentrations in winter, when compared to summer, were primarily attributed to direct fire natural gas heaters. Specific operations contributing to respirable mass elevation included pouring, abrasive blasting/grinding and melting, although many non-specific operations appeared to contribute to elevating respirable mass concentrations in all three operational areas. In addition, inadvertent recirculation of foundry process emissions appeared to play a role in ultrafine particle number and respirable mass concentration elevations for facility make-up air drawn from roof level, when compared to ambient outdoor background.

FUNDING

International Union, United Automobile, Aerospace and Agricultural Implement Workers of America (UAW); International Truck and Engine Corporation (to W.A.H. and T.M.P.).

Acknowledgements—Additional logistical support and monitoring equipment was provided by NIOSH. The cooperation of staff at the foundry and in particular the authors' primary point of contact, Sonny Painter, was greatly appreciated.

NIOSH Disclaimer—The findings and conclusions in this report are those of the authors and do not necessarily represent the views of the NIOSH. Mention of product or company name does not constitute endorsement by the Centers for Disease Control and Prevention.

REFERENCES

American Conference of Governmental Industrial Hygienists (ACGIH). (2007) 2007 TLVs and BEIs based on the documentation of the threshold limit values for chemical substances and physical agents and biological exposure indices. Cincinnati, OH: ACGIH.

American Society for Metals (ASM). (1983) ASM metals reference book. 2nd edn. Metals Park, OH: ASM.

Brook RD, Franklin B, Cascio W *et al*. (2004) Air pollution and cardiovascular disease: a statement for healthcare professionals from the Expert Panel on Population and Prevention Science of the American Heart Association. Circulation; 109: 2655–71.

Brouwer DH, Gijsbers JHJ, Lurvink MWM. (2004) Personal exposure to ultrafine particles in the workplace: exploring sampling techniques and strategies. Ann Occup Hyg; 48: 439–53.

Chang M-CO, Chow JC, Watson JG *et al*. (2005) Characterization of fine particulate emissions from casting processes. Aerosol Sci Technol; 39: 947–59.

Dasch J, D'Arcy J, Gundrum A *et al*. (2005) Characterization of fine particles from machining in automotive plants. J Occup Environ Hyg; 2: 609–25.

Dockery DW, Pope CA, Xu X *et al*. (1993) An association between air pollution and mortality in six US cities. N Engl J Med; 329: 1753–9.

Donaldson K, Brown D, Clouter A *et al*. (2002) The pulmonary toxicology of ultrafine particles. J Aerosol Med; 15: 213–20.

Englert N. (2004) Fine particles and human health: a review of epidemiological studies. Toxicol Lett; 149: 235.

Gebhart J. (2001) Optical direct-reading techniques: light intensity systems. In Baron PA and Willeke K, editors. Aerosol measurement-principles, techniques, and applications. New York: Wiley-Interscience. pp. 419–454.

Gilmour PS, Ziesenis A, Morrison ER *et al*. (2004) Pulmonary and systemic effects of short-term inhalation exposure to ultrafine carbon black particles. Toxicol Appl Pharmacol; 195: 35.

Gulijk VC, Marijnissen JCM, Makkee M *et al*. (2004) Measuring diesel soot with a scanning mobility particle sizer and an electrical low-pressure impactor: performance assessment with a model for fractal-like agglomerates. J Aerosol Sci; 35: 633–55.

Heitbrink WA, Evans DE, Peters TM *et al*. (2007) The characterization and mapping of very fine particles in an engine machining and assembly facility. J Environ Occup Hyg; 4: 341–51.

Kinsey JS, Mitchell WA, Squier WC *et al*. (2006) Evaluation of methods for the determination of diesel-generated fine particulate matter: physical characterization results. J Aerosol Sci; 37: 63–87.

Maricq MM, Ning X, Chase RE. (2006) Measuring particle mass emissions: the electrical low pressure impactor. Aerosol Sci Technol; 40: 68–79.

Maricq MM, Podsiadlik DH, Chase RE. (2000) Size distributions of motor vehicle exhaust PM: a comparison between ELPI and SMPS measurements. Aerosol Sci Technol; 33: 239–60.

Maynard AD. (2003) Estimating aerosol surface area from number and mass concentration measurements. Ann Occup Hyg; 47: 123–44.

Möhlmann C. (2005) Vorkommen ultrafeiner Aerosole an Arbeitsplätzen. Gefahrstoffe Reinhalt; 65: 469–71. Available at: http://www.hvbg.de/d/bia/pub/grl/2005_196.pdf. Accessed 17 November 2007.

National Institute for Occupational Safety and Health (NIOSH). (1998) Method 0600 particles not otherwise regulated—respirable. In Cassinelli ME and Fey-O'Connor P, editors. NIOSH manual of analytical methods. 4th edn. Cincinnati, OH: NIOSH.

Nel A. (2005) Air pollution-related illness: effects of particles. Science; 308: 804–6.

Oberdörster G. (2001) Pulmonary effects of inhaled ultrafine particles. Int Arch Occup Environ Health; 74: 1–8.

Oberdorster G, Sharp Z, Atudorei V *et al*. (2002) Extrapulmonary translocation of ultrafine carbon particles following whole-body inhalation exposure of rats. J Toxicol Environ Health A; 65: 1531–43.

Peters TM, Heitbrink WA, Evans DE *et al*. (2006) The mapping of fine and ultrafine particles in an engine machining and assembly facility. Ann Occup Hyg; 50: 249–57.

Ramachandran G, Paulsen D, Watts W *et al*. (2005) Mass, surface area and number metrics in diesel occupational exposure assessment. J Environ Monit; 7: 728–35.

Riediger G, Möhlmann C. (2001) Ultrafeine Aerosole an Arbeitsplätzen—Konventionen und Beispiele aus der Praxis. Gefahrstoffe Reinhalt; 61: 429–34. Available at: http://www.hvbg.de/d/bia/pub/grl/065_2001.pdf. Accessed 17 November 2007.

Samet JM, Dominici F, Curriero FC *et al*. (2000) Fine particulate air pollution and mortality in 20 U.S. cities, 1987–1994. N Engl J Med; 343: 1742–9.

Thomassen Y, Koch W, Dunkhorst W *et al*. (2006) Ultrafine particles at workplaces of a primary aluminium smelter. J Environ Monit; 8: 127–33.

TSI. (2004) Model 3007 Hand-held condensation particle counter specifications. Available at: http://www.tsi.com/documents/3007.pdf. Accessed 17 November 2007.

Vincent JH, Clement CF. (2000) Ultrafine particles in workplace atmospheres. R Soc; 358: 2673–82.

Zimmer AT, Biswas P. (2001) Characterization of the aerosols resulting from arc welding processes. J Aerosol Sci; 32: 993–1008.

Zimmer AT, Maynard AD. (2002) Investigation of the aerosols produced by a high-speed hand-held grinder using various substrates. Ann Occup Hyg; 46: 663–72.